Heliyon 11 (2025) e41594

Contents lists available at ScienceDirect

Heliyon

journal homepage: www.cell.com/heliyon

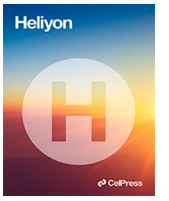

Research article

Identification of RAD51AP1 as a key gene in hepatitis B virus-associated hepatocellular carcinoma

Meiling Wan [a,b,1], Yonghong Wang [a,b,1], Xiaoling Liu [a,b], Yaling Li [c], Cunliang Deng [a,b,**], Changfeng Sun [a,b,*]

[a] Department of Infectious Diseases, Affiliated Hospital, Southwest Medical University, Luzhou, 646000, China
[b] Laboratory of Infection and Immunity, The Affiliated Hospital, Southwest Medical University, Luzhou, 646000, China
[c] Department of Pharmacy, The Affiliated Hospital, Southwest Medical University, Luzhou, 646000, China

ARTICLE INFO

Keywords:
RAD51AP1
HBV-Associated HCC
Prognostic biomarker
Proliferation
Metastasis

ABSTRACT

Background: Hepatocellular carcinoma (HCC) is a significant global health concern, with chronic hepatitis B virus (HBV) infection being a major contributor. Understanding the mechanisms of HBV-associated HCC is crucial to improving the prognosis and developing effective treatments.
Methods: HBV-associated HCC datasets (GSE19665, GSE121248, GSE55092, GSE94660, and TCGA-LIHC) acquired from public databases were mined to identify key driver genes by differentially expressed gene analysis, weighted gene co-expression network analysis (WGCNA), followed by protein-protein interaction network analysis, Lasso-Cox regression analysis, and randomforestSRC algorithm. Then, in vitro experiments including CCK-8 assay, wound healing, and Transwell assay were performed to explore the functions and mechanisms.
Results: RAD51AP1 was identified as a specific key gene linked to the progression of HBV-associated HCC. High expression of RAD51AP1 was associated with worse overall survival (OS) in patients with HBV-associated HCC, but not in patients with non-HBV-associated HCC. Mechanistically, RAD51AP1 forms a potential ceRNA axis with LINC01419 and miR-8070, where LINC01419 acts as a molecular sponge for miR-8070 to upregulate RAD51AP1. HBV infection can enhance the LINC01419/miR-8070/RAD51AP1 axis, and LINC01419 overexpression conversely promotes HBV replication. The ceRNA axis and HBV synergistically promote the proliferation and metastasis of HBV-associated HCC cells. Furthermore, LINC01419 or RAD51AP1 knockdown, and miR-8070 overexpression in HepG2.2.15 cells significantly attenuated the Wnt/β-catenin signaling.
Conclusions: The LINC01419/miR-8070/RAD51AP1 axis promotes the HBV-associated HCC progression through an HBV-boosted positive feedback loop and Wnt/β-catenin signaling. These findings provide novel insights into the underlying mechanisms and may offer potential diagnostic and therapeutic targets in HBV-associated HCC.

* Corresponding author. Department of Infectious Diseases, Affiliated Hospital, Southwest Medical University, Luzhou, 646000, China.
** Corresponding author. Department of Infectious Diseases, Affiliated Hospital, Southwest Medical University, Luzhou, 646000, China.
E-mail addresses: dengcunl@swmu.edu.cn (C. Deng), sun_cf88@swmu.edu.cn (C. Sun).
[1] These authors contributed equally to this work.

https://doi.org/10.1016/j.heliyon.2024.e41594
Received 18 August 2024; Received in revised form 25 November 2024; Accepted 30 December 2024
Available online 31 December 2024

1. Introduction

Hepatocellular carcinoma (HCC) ranks among the most prevalent malignancies globally, with the sixth highest incidence, and is the third leading cause of cancer-related deaths (https://gco.iarc.fr/today/home) [1,2]. Chronic hepatitis B virus (HBV) infection is closely tied to the incidence and development of HCC. Approximately 50 % of HCC cases worldwide can be attributed to HBV infection [3], particularly in China, where 84 % of HCC cases are the result of HBV infection. Moreover, the prognosis of patients with HBV-associated HCC is notably poorer than that of patients with non-HBV-associated HCC [4]. Analyzing the disparities in gene expression between HBV-associated HCC tissues and adjacent normal tissues to identify key driving genes will help us deepen our understanding of the mechanisms of HBV-associated HCC progression and may offer potential targets for the treatment of HBV-associated HCC. However, the mechanisms through which HBV infection drives the progression of HBV-associated HCC have not been fully clarified.

The development of high-throughput analytical techniques and bioinformatics has unlocked the potential for comprehensive screening of novel and potential biomarkers. Public databases such as the Cancer Genome Atlas (TCGA, https://portal.gdc.cancer.gov/) and Gene Expression Omnibus (GEO, http://www.ncbi.nlm.nih.gov/geo/) contain numerous transcriptome expression profiles and clinical information, facilitating the screening of differentially expressed genes (DEG) associated with HCC carcinogenesis and progression. Recently, Qiang R et al. [5]; Ding W et al. [6]; Wang S Y et al. [7]; Liu, C. et al. [8]; Sha M et al. [9]; Zheng H et al. [10] identified key genes associated with the poor prognosis or immune microenvironment of HBV-associated HCC through DEGs analysis or weighted gene co-expression network analysis (WGCNA). In this study, we recharacterized the key driver genes of HBV-associated HCC by combining different datasets with DEGs analysis and WGCNA, followed by protein-protein interaction (PPI) network analysis, Lasso-Cox regression analysis, and randomForestSRC algorithm to identified those that had significant impacts on the prognosis of patients with HBV-associated HCC. Ultimately, the latter three methods collectively showed that RAD51AP1 has a significant effect on the prognosis of patients with HBV-associated HCC. In the previous study, Wei Y G et al. considered RAD51AP1 as an immunologically related prognostic biomarker and a predictor of response to treatment in patients with HCC [11]. Here, we performed a subgroup analysis to assess the influence of RAD51AP1 on the prognosis of patients with HBV-associated or non-HBV-associated HCC and discovered that RAD51AP1 was associated with overall survival (OS) and disease-free interval (DFI) only in patients with HBV-associated HCC. Therefore, we hypothesized that RAD51AP1 might play a specialized critical role in HBV-associated HCC, which remains ambiguous. This study aimed to investigate the difference in clinical relevance of RAD51AP1 in patients with HBV-associated HCC and non-HBV-associated HCC and to elucidate the mechanism by which RAD51AP1 promotes the progression of HBV-associated HCC, which may facilitate a deeper understanding of the mechanisms of HBV-associated HCC progression and provide a prognostic marker specific for patients with HBV-associated HCC.

2. Material and methods

2.1. Data collection

Four HBV-associated HCC datasets, namely GSE19665, GSE121248, GSE55092, and GSE94660, were downloaded from the GEO database (https://www.ncbi.nlm.nih.gov/geo/). Datasets from the same platform were merged using the “sva” package in R version 4.3 (The R Foundation for Statistical Computing, Austria). The “combat” function was utilized to remove the batch effect. Furthermore, RNA-seq data from HCC patients and the corresponding clinical information in the TCGA-LIHC database were acquired from the UCSC Xena website (https://xena.ucsc.edu/). In the TCGA cohort, patients with the inclusion criteria of positive HBsAg or HBV DNA were considered to have HBV-associated HCC. GSE14520 in the GEO database, and LIRI-JP in the International Cancer Genome Consortium (ICGC, https://dcc.icgc.org/) served as the validation cohort. Detailed information on the datasets is provided in Supplementary Table S1.

2.2. Identification of differentially expressed genes

The “limma” package in R was employed to identify DEGs between HBV-associated HCC and paracancerous tissues based on predefined criteria. The criteria for DEGs were as follows: the absolute value of the log2FC was greater than 1, and the adjusted p-value was less than 0.05.

2.3. Weighted correlation network analysis (WGCNA)

Weighted correlation network analysis is capable of clustering genes with similar expression patterns and uncovering associations between genes and phenotypes within a module, which will assist us in finding the hub genes. In this study, the "WGCNA" package in R was utilized to construct gene co-expression networks to identify modules and pivotal genes related to HBV-associated HCC.

2.4. Cell culture and transfection

The human HCC cell lines HepG2-NTCP and HepAD38 were procured from Qingqi Biotechnology Development Co., Ltd. (Shanghai, China). HepG2 was obtained from Procell Life Science & Technology Co., Ltd. (Wuhan, China), and HepG2.2.15 was bought from iCell Bioscience Inc. (Shanghai, China). HCC cells were cultivated in a humidified incubator at 37 °C and 5 % CO2. Dulbecco’s modified

Eagle's medium (DMEM) was used for HepG2, HepG2.2.15, and HepG2-NTCP cells, and minimum essential medium (MEM) was used for HepAD38 cells. The culture media were supplemented with 10 % fetal bovine serum (FBS). Penicillin (100 IU/ml) and streptomycin (100 mg/ml) were added as necessary. The characteristics of the HCC cells used in this study are listed in Supplementary Table S2. Cell transfection was carried out using the Lipofectamine™ 3000 Transfection Reagent (L3000015, Invitrogen, USA) following the manufacturer's instructions. The sequences of siRNAs and miRNA mimics used in the study are listed in Supplementary Table S3.

2.5. Real-time quantitative PCR

Total RNA was extracted from tissues and cells using Trizol regent (EX1880, G-CLONE, China). 2 μg total RNA was reverse transcribed into cDNA using an RNA reverse transcription kit. The qRT-PCR reaction system was prepared following the instructions of the qRT-PCR reaction kit, and the relative expression of genes of interest was calculated using the -ΔΔCt method. All reagents were purchased from Servicebio Biotech Co., Ltd. (Wuhan, China). The sequences of primers used in the study are listed in Supplementary Table S4.

2.6. Western blotting

Proteins were extracted using a protein extraction kit (KGP150, Keygen, China), separated by sodium dodecyl sulfate-polyacrylamide gel electrophoresis (SDS-PAGE), and then transferred to a polyvinylidene difluoride (PVDF) membrane. The membrane was blocked with 5 % skimmed milk for 2 h at room temperature and subsequently incubated with primary antibodies overnight at 4 °C, followed by incubation with secondary antibodies (1:3000) for an hour at room temperature. Finally, a supersensitive ECL chemiluminescent substrate (BL520A, Biosharp, China) was added to detect protein bands using a chemiluminescence imaging system. The relative quantification of protein bands of interest was calculated using ImageJ software. The antibodies used for the western blotting assay are listed in Supplementary Table S5.

2.7. Dual-luciferase reporter assay

The pmiR-RB-Reporter assay system was employed to detect miRNA binding activity to target genes. hRluc and hluc functioned as the reporter gene and reference gene, respectively. The pRB-LINC01419-WT and pRB-RAD51AP1-WT harbor the predicted wild-type binding sequences of the target gene mRNAs, and the pRB-LINC014-MUT and pRB-RAD51AP1-MUT contain the corresponding mutated sequences, respectively. In the dual-luciferase reporter gene assay, HCC cells were co-transfected with recombinant pmiR-RB-Reporter vector and miR-8070 mimics, and the fluorescence intensity was determined using a dual-luciferase reporter assay kit (KGE3302, Keygen, China) after 24 h. All vectors were constructed by Ribobio Co., LTD. (Guangzhou, China). The plasmids used in this study are listed in Supplementary Table S6.

2.8. Cell-counting Kit-8 assay

HCC cells were inoculated in 96-well plates in five replicates at a density of 3×10^3 cells/well. At 0, 24, 48, 72, and 96 h, 10 μl cell counting kit-8 (CCK-8) reagent (GK10001, Glpbio, USA) was added to each well and incubated for 3 h. The absorbance at 450 nm was measured using a microplate reader.

2.9. Transwells assay

HCC cells were seeded in the upper chamber at a density of 5 × 104 cells/well. For the invasion assay, the upper chamber was precoated with 50 μl of 3 mg/ml Matrigel. The lower chamber was filled with 600 μl DMEM supplemented with 10 % FBS. After 48 h, cells were fixed with 4 % paraformaldehyde solution for 30 min and stained with 0.1 % crystal violet for 30 min. The non-transferred cells were wiped away with a cotton swab, and ten fields (100 ×) were randomly selected in different regions of the Transwell chamber under a microscope to count migrated and invaded cells.

2.10. Scratch assay

HCC cells were inoculated in a 24-well cell culture plate at a density of 2×10^5 cells/well. When cell confluence reached 80 %–90 %, a 200 μl sterile pipette tip was used to scratch the cell monolayer. After being rinsed three times with phosphate buffer solution (PBS), images (40 ×) of the scratches at 0 and 48 h were captured using an inverted microscope. The wound closure rate was measured using ImageJ software to evaluate cell migration ability.

2.11. Cell cycle analysis

HCC cells were trypsinized, washed once with PBS, and fixed with 75 % ethanol at −20 °C overnight. After centrifugation to remove the ethanol, PBS was added to rehydrate the cells at room temperature for 15 min. The cells were then stained with propidium Iodide (PI) solution (supplemented with 2.5 mg/ml RNase A) and subsequently analyzed using a flow cytometer to determine the proportion of cells in different phases of the cell cycle.

2.12. EdU incorporation assay

HCC cells were inoculated into 24-well cell culture plates at a density of 1 × 105 cells/well and cultured overnight. 5-ethynyl-2-deoxyuridine (EdU) incorporation assay was performed according to the instructions of an EdU Cell Replication Kit (E607204, Sangon Biotech., China). Briefly, cells were labeled with EdU for an appropriate time (1/5 to 1/10 of the cell cycle), followed by fixation with paraformaldehyde, staining with TAMRA, and Hoechst 33342 at room temperature in the dark. Finally, EdU-positive cells were detected under an inverted fluorescence microscope.

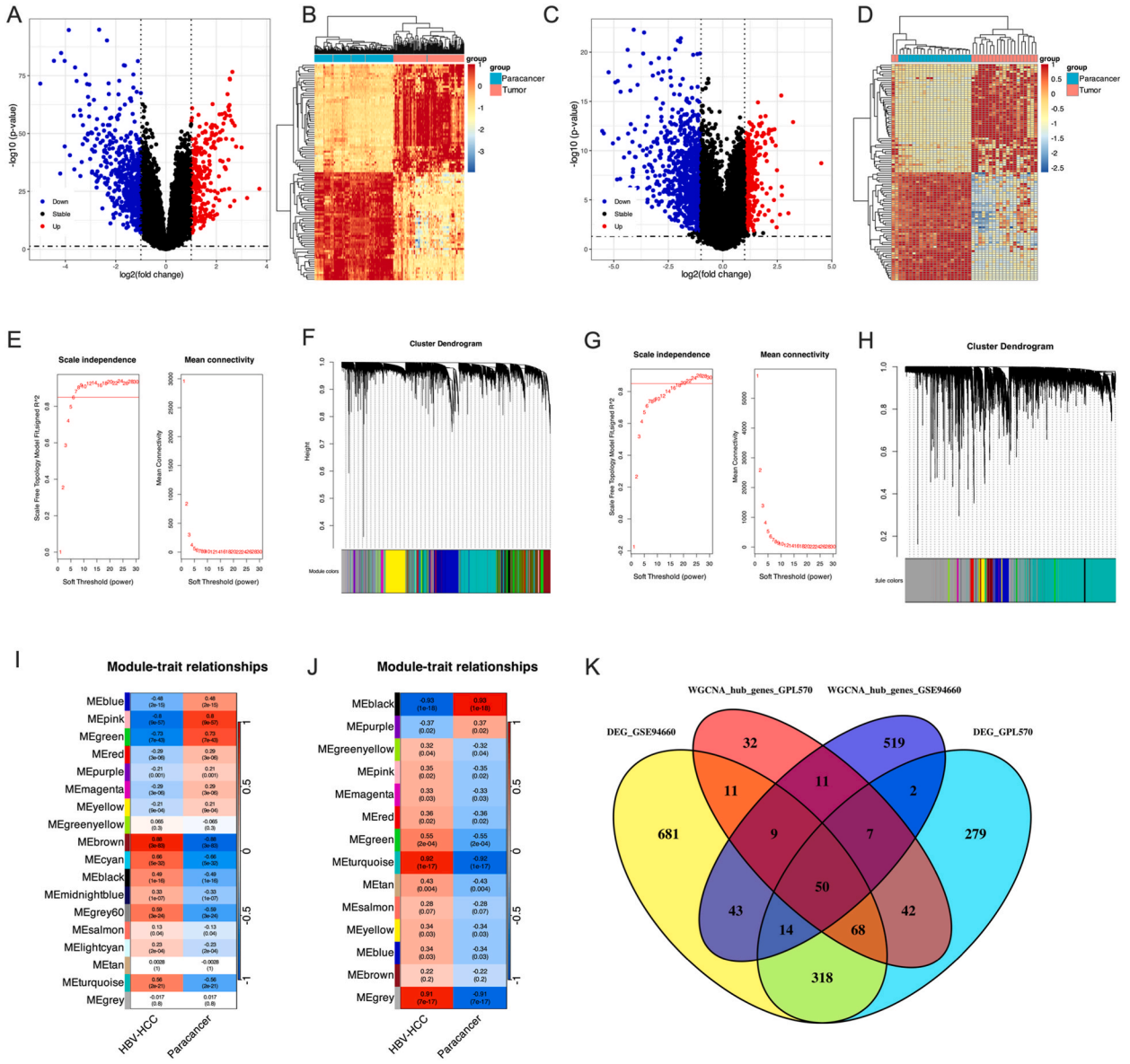

Fig. 1. Identification of differentially expressed genes and co-expression modules associated with the clinical features in the GEO datasets. (A–B) Volcano plot and heatmap of differentially expressed RNAs in the GPL570_data, where red represents the upregulated genes and blue represents the downregulated genes in the volcano plot; (C, D) Volcano plot and heatmap of differentially expressed RNAs in the GSE94660 dataset, where red represents the upregulated genes and blue represents the downregulated genes in the volcano plot; (E) Analysis of the scale-free fit index and mean connectivity for various soft-thresholding powers based on GPL570_data; (F) Dendrogram of all genes clustered in the GPL570_data; (G) Analysis of the scale-free fit index and mean connectivity for various soft-thresholding powers based on GSE94660; (H) Dendrogram of all genes clustered in the GSE94660 dataset; (I, J) Correlation between modules and clinical features in the GPL570_data and GSE94660, respectively. Each cell contains the corresponding correlation coefficient (the upper number) and the P-value (the lower number); (K) The Venn diagram showing the intersection of DEGs and co-expression modules.

3. Statistical analysis

Data are presented as mean ± standard deviation (mean ± SD), and analyses were performed using SPSS 23.0 (IBM Corp, USA) and GraphPad Prism 10.0 software (GraphPad Software, Inc., USA). Comparisons between groups were performed using t-tests or analysis of variance (ANOVA). Kaplan-Meier survival analyses were performed using the "survival" and "survminer" packages, Lasso-Cox regression using the "glmnet" package, and random forest survival analysis using the "randomForestSRC" package in R 4.3. Each experiment was replicated three times independently. The significance level was established at $p < 0.05$.

4. Results

4.1. The core key genes related to HBV-associated HCC

Three datasets (GSE19665, GSE121248, and GSE55092) generated from the GPL570 platform (HG-U133_Plus_2) were merged with the "sva" package in R, named GPL570_data. Based on the GPL570_data, 252 up-regulated and 528 down-regulated genes were filtered using the "limma" package in R, including 11 differentially expressed lncRNA (DElncRNA) (Fig. 1A and B). GSE94660 was generated from the GPL16791 Illumina HiSeq 2500 (Homo sapiens) platform, and 1194 DEGs were identified, consisting of 319 up-regulated

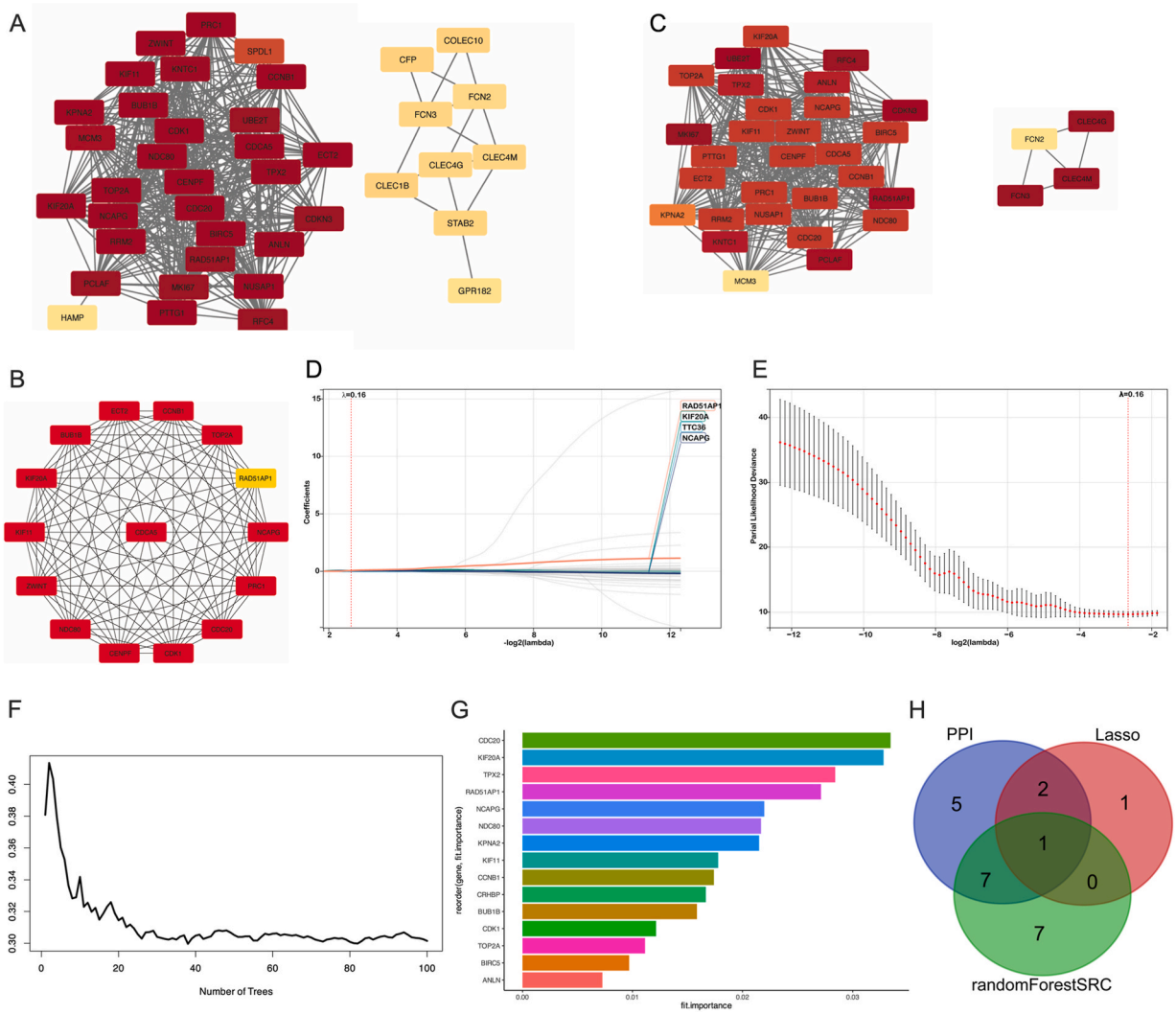

Fig. 2. Selection of the feature genes related to HBV-associated HCC. (A) Protein-protein interaction (PPI) network of hub genes; (B) The top 15 hub genes in the PPI network were extracted by the degree algorithm of the cytoHuhabb plugin in Cytoscape 3.8 software; (C) The key modules of the PPI network were identified by the MOCDE plugin in Cytoscape 3.8 software; (D, E) Adjustment of feature selection in the least absolute shrinkage and selection operator (LASSO) and cox regression analysis; (F, G) The top15 important genes associated with OS in patients with HBV-associated HCC screened by the randomForestSRC algorithm; (G) Venn diagram screening of feature genes obtained by the three algorithms.

genes and 875 down-regulated genes (Fig. 1C and D). Additionally, GPL570_data and GSE94660 underwent WGCNA analysis to construct gene co-expression networks (Fig. 1E–H). For the GPL570_data, the brown and pink modules, and for the GSE94660 dataset, the black, turquoise, and gray modules were closely related to the HBV-associated HCC (Fig. 1I and J). 230 and 655 hub genes were obtained from GPL570_data and GSE94660, respectively, using WGCNA. Then 50 overlapping genes in the four gene sets were identified using the Venn diagram (Fig. 1K).

Subsequently, a PPI network was constructed to illustrate the interaction between the 50 hub genes (Fig. 2A). By using the degree algorithm of the cytoHubabb plugin in Cytoscape 3.8, the top 15 hub genes in the PPI network were extracted (Fig. 2B), all of which were distributed in the key modules identified by the MCODE plugin(Fig. 2C). To further screen for genes associated with prognosis in patients with HBV-associated HCC, 133 HBV-associated HCC patients were recruited from the TCGA-LIHC database. Using Lasso-Cox regression (Fig. 2D and E) and the randomForestSRC algorithm (Fig. 2F and G), 4 and 15 important genes were filtered, respectively. Finally, we selected the intersecting genes from the three methods as the core key genes related to HBV-associated HCC, and only RAD51AP1 was retained (Fig. 2H). Furthermore, we also analyzed the effect of the top 15 genes screened by PPI analysis on OS of

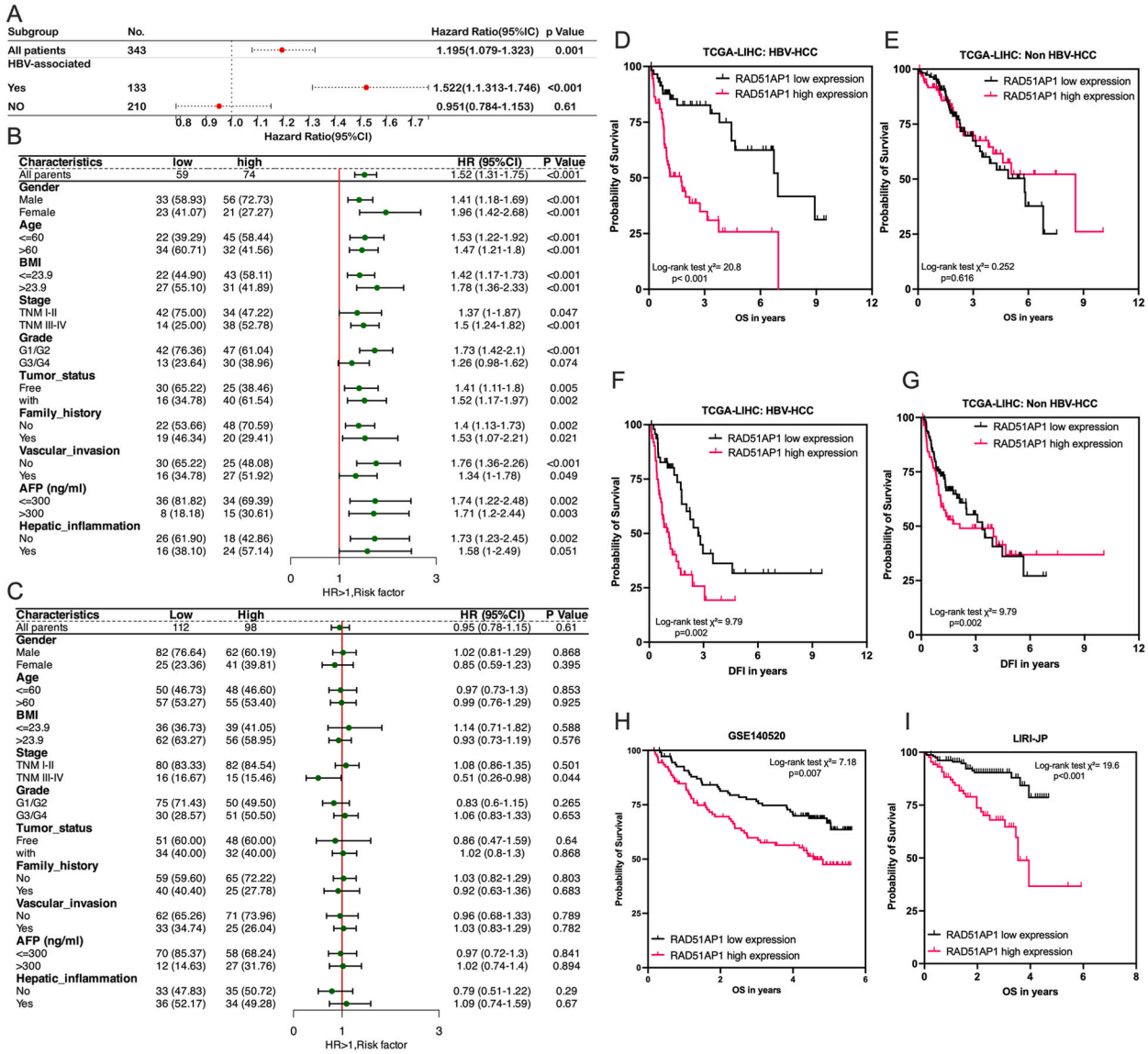

Fig. 3. Subgroup analysis of the correlation between RAD51AP1 expression and clinical characteristics. (A) Cox regression analysis of RAD51AP1 on overall survival (OS) in the patients with HBV-associated HBV or non-HBV-associated HCC; (B, C) Cox subgroup analysis of RAD51AP1 and clinical characteristics in patients with HBV-associated HCC and non-HBV-associated HCC, respectively; (D, E) OS curves of patients with HBV-associated HCC or non-HBV-associated HCC with high and low expression of RAD51AP1 in the TCGA cohort; (F, G) Disease-free interval (DFI) curves of patients with HBV-associated HCC or non-HBV-associated HCC with high and low expression of RAD51AP1 in the TCGA cohort; (H–I) OS curves of HBV-associated HCC patients with high and low expression of RAD51AP1 in the validation cohorts GSE14520 and LIRI-JP.

patients with HBV-associated HCC. As shown in Supplementary Fig. S1, the top 15 hub genes were highly expressed in HBV-associated HCC tissues, and were risk factors associated with worse OS in patients with HBV-associated HCC. Cox regression analysis demonstrated that among the top 15 hub genes, RAD51AP1 had the largest hazard ratio (HR) for patients with HBV-associated HCC (HR = 1.522, 95%IC: 1.313–1.764). Together, RAD51AP1 may be a core key gene associated with the prognosis of patients with HBV-associated HCC.

4.2. *RAD51AP1 served as a prognosis biomarker in HBV-associated HCC patients*

By Cox regression analysis, the HR of RAD51AP1 was calculated separately for the patients with HBV-associated HCC or non-HBV-

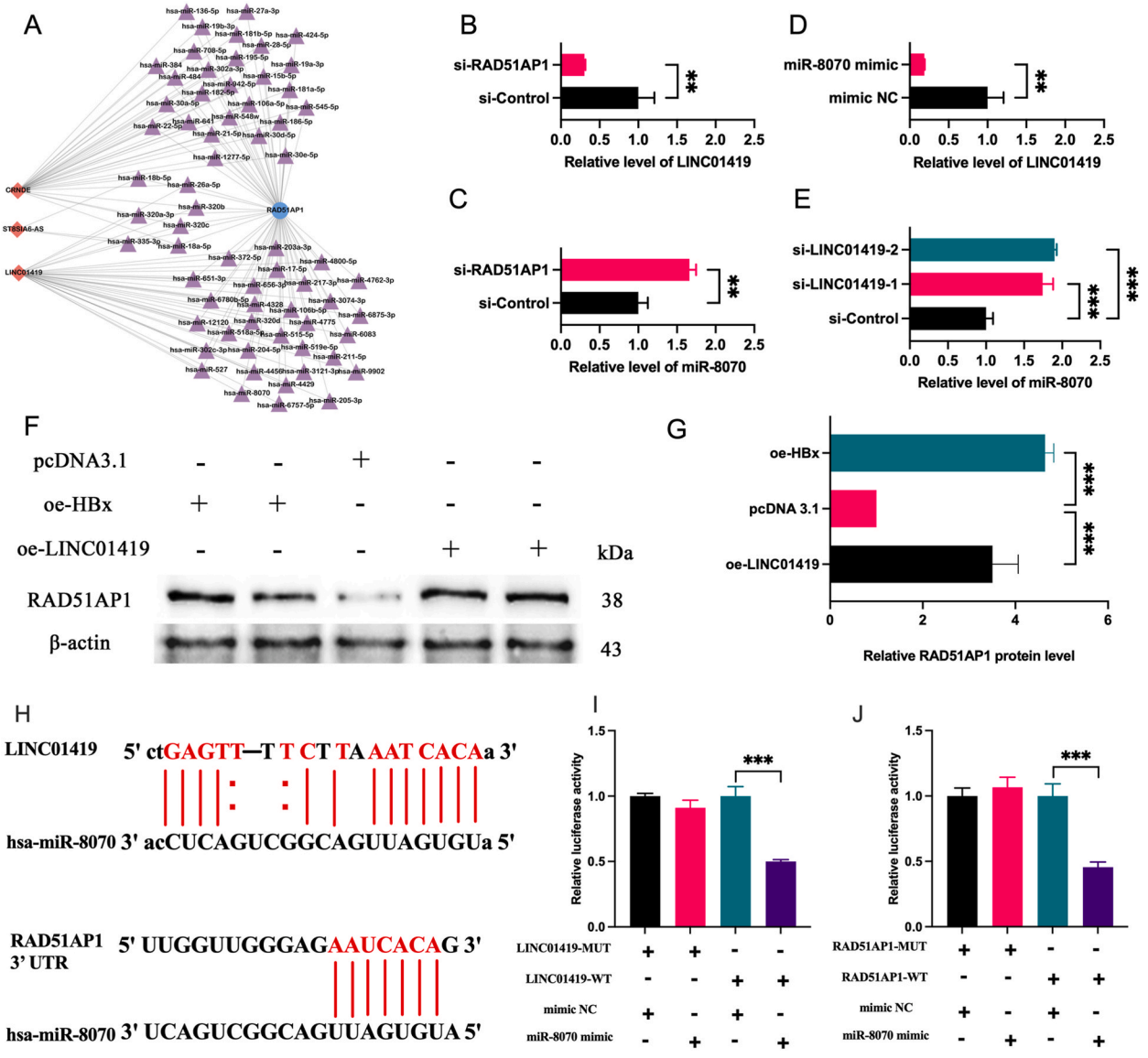

Fig. 4. Validation of the LINC01419/miR-8070/RAD51ap1 ceRNA network. (A) The ceRNA network involved in RAD51AP1 was constructed using Cytoscape software; (B, C) The expression of LINC01419 and miR-8070 in the HepG2.2.15 transfected with siRNA si-RAD51AP1; (D) the expression of LINC01419 in the HepG2.2.15 transfected with miR-8070 mimic; (E) The expression of miR-8070 in the HepG2.2.15 transfected with si-LINC01419; (F–G) The expression of RAD51AP1 in the HepG2.2.15 transfected with overexpression vector oe-LINC01419 or oe-HBx, detected by Western blotting; (H) The predicted binding sites of miR-8070 in LINC01419 and the 3′-UTR of the RAD51AP1 mRNA; (I–J) Results of the dual luciferase reporter assay. Dual luciferase reporter assays were performed to examine the interaction of miR-8070 and its targeting sequence in the LINC01419 and the 3′-UTR of the RAD51AP1 mRNA using constructs containing the targeting sequence (termed -WT) and mutated targeting sequence (termed -MUT) cloned into the pmiR-RB-Report™ vector, the Renilla luciferase (hRluc) activity was normalized to luciferase (hluc) activity. *P < 0.05; **P < 0.01; ***P < 0.001; ns: No statistically significant difference.

associated HCC, and RAD51AP1 acted as a risk factor only in patients with HBV-associated HCC (Fig. 3A). To further explore the clinical correlation between RAD51AP1 and HBV-associated HCC, we conducted subgroup analyses based on data from the TCGA-LIHC database. Using the median of RAD51AP1 expression as a cutoff value, 343 HCC patients (133 HBV-associated HCC and 210 non-HBV-associated HCC) with complete survival information (OS $\geq$ 30 days) and gene expression data in the TCGA-LIHC database were classified into high- and low-expression groups. Among 133 HBV-associated HCC patients, 59 and 74 patients were classified into the low and high RAD51AP1 expression groups, respectively. Of the 210 patients with non-HBV-associated HCC, 112 patients were assigned to the low RAD51AP1 expression group and 98 patients to the high RAD51AP1 expression group. Cox regression subgroup analysis of the correlation between RAD51AP1 expression and clinical indicators in various patient categories revealed that RAD51AP1 served as a risk factor in patients with HBV-associated HCC with different gender, age, BMI, TNM stage, family history, etc., whereas it scarcely served as a risk factor or protective factor in patients with non-HBV-associated HCC with different clinical indicators (Fig. 3B and C). Kaplan-Meier survival analysis indicated a significant correlation between RAD51AP1 expression and OS and

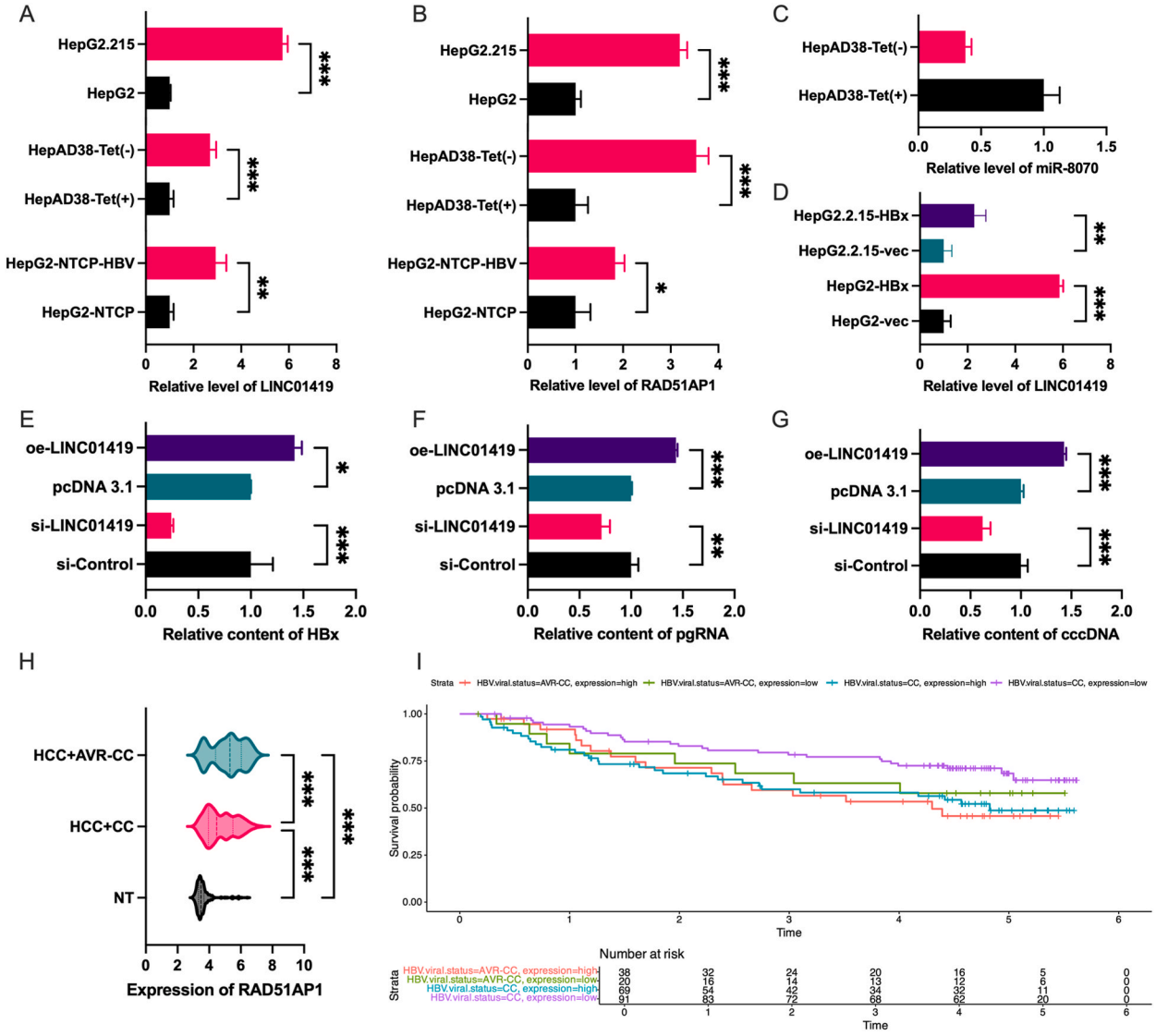

Fig. 5. Correlation between the expression of LINC01419/miR-8070/RAD51AP1 axis and HBV infection. (A) Relative expression of LINC01419 in three pairs of HCC cells: HepG2.2.15 vs HepG2, HepAD38-Tet (−) vs HepAD38-Tet (+) and HepG2-NTCP-HBV vs HepG2-NTCP; (B) Relative expression of RAD51AP1 in three pairs of HCC cells: HepG2.2.15 vs HepG2, HepAD38-Tet (−) vs HepAD38-Tet (+) and HepG2-NTCP-HBV vs HepG2-NTCP; (C) The relative expression of miR-8070 in HepAD38 Tet (−) and HepAD38 Tet (+) cells; (D) The relative expression of LINC01419 in HepG2.2.15 and HepG2 transfected with overexpression vector oe-HBx; (E–G) The levels HBx (E), pgRNA (F), and cccDNA (G) in the nucleus in HepG2.2.15 transfected with the overexpression vector oe-LINC01419 or siRNA si-LINC01419; (H) The expression of RAD51AP1 in HBV chronic carriers (CC) and active viral replication chronic carriers (AVR-CC) with HBV-associated HCC in the GSE14520 dataset. (I) OS curves of CC and AVR-CC with HBV-associated HCC with different expression levels of RAD51AP1 in the GSE14520 dataset. *P < 0.05; **P < 0.01; ***P < 0.001.

DFI in patients with HBV-associated HCC, whereas RAD51AP1 was not significantly correlated with OS and DFI in patients with non-HBV-associated HCC (Fig. 3D–G). To validate the association of RAD51AP1 with OS in patients with HBV-associated HCC, we utilized the GSE14520, and LIRI-JP as validation cohorts. As shown in Fig. 3H and I, patients with high expression of RAD51AP1 had poorer OS in the two datasets.

4.3. The ceRNA network involved in RAD51AP1 in HBV-associated HCC

To understand the mechanism of RAD51AP1 in HBV-associated HCC, we constructed a ceRNA network related to the gene. As mentioned above, 11 DElncRNAs were screened in the GPL570_data, among which three lncRNAs were found to be up-regulated, namely CRNDE, LINC01419, and ST8SIA6-AS1. The interactions of RAD51AP1, CRNDE, LINC01419, and ST8SIA6-AS1 with potential miRNAs were predicted in miRDB, ENCORI, targetScan, miRtarBase and LncBase, and a ceRNA network was constructed in Cytoscape software 3.8 (Fig. 4A). The LINC01419/miR-8070/RAD51AP1 axis in HBV-associated HCC remains ambiguous. Subsequently, we first examined the expression correlation of three genes in HepG2.2.15 cells. As indicated by the qPCR results, the

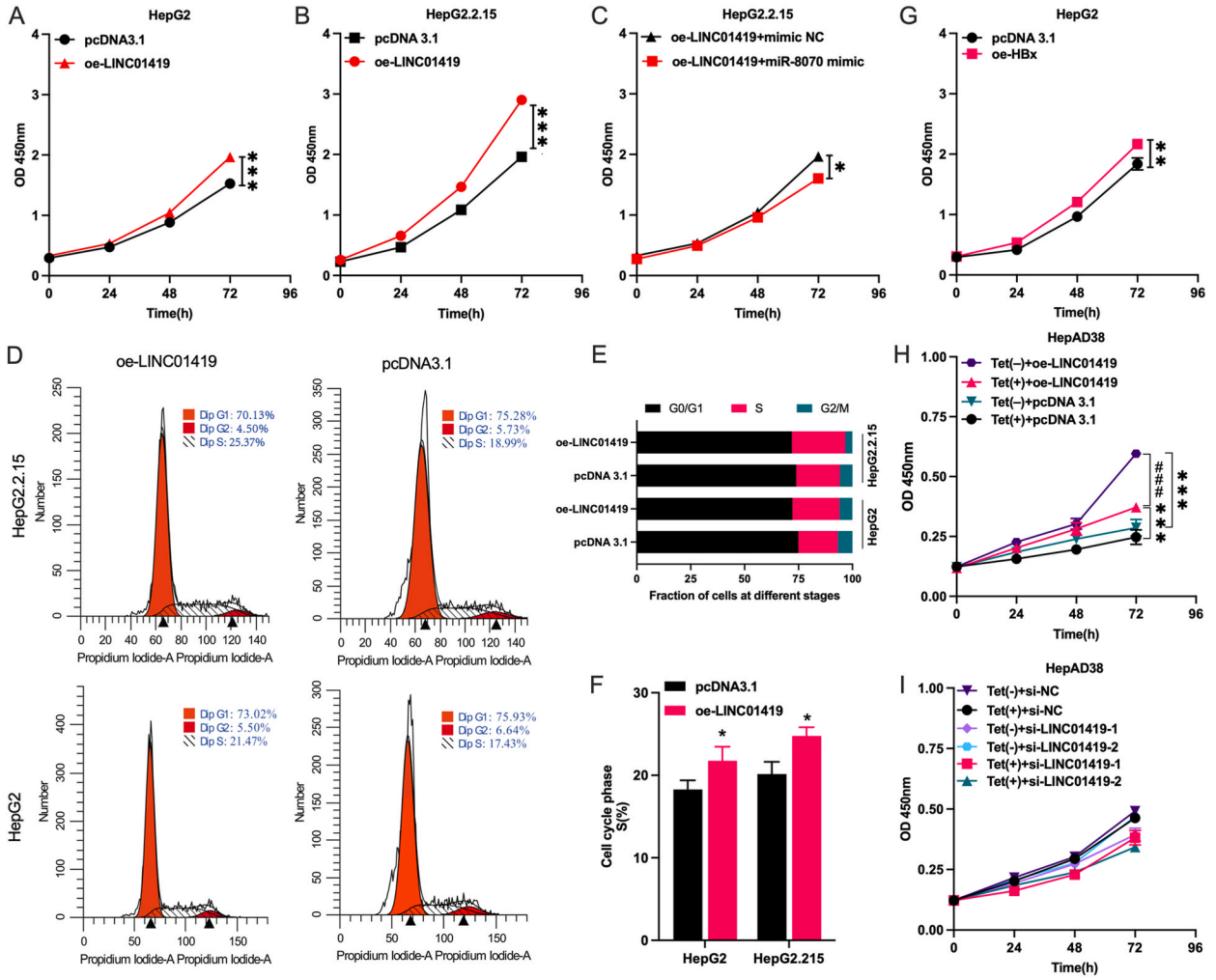

Fig. 6. The synergistic effect of LINC01419 and HBV on cell proliferation. (A, B) CCK8 assay showing the effect of LINC01419 overexpression on the proliferation of HepG2 and HepG2.2.15 compared with that of cells transfected with vehicle vector; (C) CCK8 assay showing the effect of miR-8070 mimic on proliferation of LINC01419 overexpressed HepG2.2.15 cells compared to that of cells transfected with mimic NC; (D) Flow cytometry analysis showing the cell cycle of HepG2.2.15 and HepG2 cells transfected with oe-LINC01419 or vehicle vector; (E) Proportion of cells in different phases of HepG2.2.15 and HepG2 cells transfected with oe-LINC01419 or vehicle vector; (F) Proportion of cells in S phase of HepG2.2.15 and HepG2 cells transfected with oe-LINC01419 or vehicle vector; (G) CCK8 assay showing the effect of HBx on the proliferation of HepG2 cells compared to that of cells transfected with vehicle vector; (H) CCK8 assay showing the effect of LINC01419 overexpression on the proliferation of HepAD38 Tet (−) and HepAD38 Tet (+) cells compared to that of cells transfected with vehicle vector; (I) CCK8 assay showing the effect of LINC01419 knockdown on the proliferation of HepAD38 Tet (−) and HepAD38 Tet (+) cells compared to that of cells transfected with siRNA NC. *P < 0.05; **P < 0.01; ***P < 0.001.

knockdown of RAD51AP1 resulted in decreased expression of LINC01419 and increased expression of miR-8070 (Fig. 4B and C). Overexpression of miR-8070 significantly decreased the expression of LINC01419 (Fig. 4D), whereas knockdown of LINC01419 increased the expression of miR-8070 (Fig. 4E). Western blot analysis demonstrated that overexpression of LINC01419 in HepG2.2.15 cells resulted in up-regulation of RAD51AP1 expression (Fig. 4F and G). Further dual luciferase reporter assays revealed that the relative fluorescence intensity was significantly reduced in the miR-8070 mimic and pRB-RAD51AP1-WT (or pRB-LINC01419-WT) co-transfection group compared to the miR-8070 mimic NC and pRB-RAD51AP1-WT (or pRB-LINC01419-WT) co-transfection group, while there was no significant difference in the relative fluorescence intensity between the miR-8070 and pRB-RAD51AP1-MUT (or pRB-LINC01419-MUT) co-transfection group and the miR-8070 mimic NC and pRB-RAD51AP1-MUT (or pRB-LINC01419-MUT) co-transfection group(Fig. 4H–J). Collectively, this suggests that miR-8070 may inhibit the expression of LINC01419 and RAD51AP1 by directly targeting LINC01419 and 3′UTR of the RAD51AP1 mRNAs.

4.4. HBV enhances the LINC01419/miR-8070/RAD51AP1 axis in HBV-associated HCC

To determine whether the expression of the LINC01419/miR-8070/RAD51AP1 axis is associated with HBV infection in HBV-associated HCC, we performed the analysis in three pairs of cells, namely: HepG2.2.15 vs HepG2, HepAD38 Tet (−) vs HepAD38 Tet (+), and HepG2-NTCP-HBV vs HepG2-NTCP. Here, HepG2.2.15 cells are a stable cell line that integrates two copies of the HBV genome in HepG2 cells, capable of stably expressing viral protein and ensuring sustained HBV replication capacity. The HepAD38 Tet-off cell line (−) can replicate HBV in the absence of tetracycline (Tet) in growth media, and the production of HBV and the intracellular accumulation of covalently closed circular DNA (cccDNA) are significantly higher than in HepG2.2.15. HepG2-NTCP-HBV was derived from HepG2-NTCP, which was *de novo* infected with HBV according to previous studies [12], with slight modifications. As shown in Fig. 5A–C, both LINC01419 and RAD51AP1 were significantly up-regulated in HepG2.2.15, HepAD38 Tet (−), and HepG2-NTCP-HBV cells compared to their respective control cells, whereas miR-8070 expression levels were significantly downregulated in the HepAD38 Tet (−) cells. HBx, the smallest open reading frame (ORF) in the HBV genome, is a multifunctional viral regulator that influences cell cycle regulation and apoptosis by modulating cellular and viral transcriptional activities, signaling pathways, genotoxic stress responses, and protein degradation. HBx may play an initiating role in tumorigenesis in chronic active hepatitis and cirrhosis. In the current study, overexpression of HBx in HepG2.2.15 and HepG2 cells also significantly increased the expression of RAD51AP1 and LINC01419 (Fig. 4F–G, Fig. 5D), suggesting that HBV may enhance the LINC01419/miR-8070/RAD51AP1 axis through HBx. In turn, LINC01419 overexpression in HepG2.2.15 cells increased HBx and pregenomic RNA (pgRNA) levels, as well as HBV cccDNA levels in the nucleus (Fig. 5E–G), and knockdown of LINC01419 led to opposite results (Fig. 5E–G). These results suggest that overexpressed LINC01419 may promote HBV replication.

To further investigate the effect of HBV viral status on RAD51AP1 expression levels, we compared the disparities in RAD51AP1 expression between HBV chronic carriers (CC) and active viral replication chronic carriers (AVR-CC) in the GSE14520 dataset. Here, both CC and AVR-CC suffered from HBV-associated HCC. As shown in Fig. 5H, RAD51AP1 was significantly up-regulated in CC and AVR-CC compared to non-tumor tissues, and RAD51AP1 expression in AVR-CC was significantly higher than in CC, suggesting that high expression of RAD51AP1 may be associated with active replication of HBV. Kaplan-Meier survival analysis revealed that there was a significant difference in prognosis between patients with CC with high or low expression of RAD51AP1, while the expression level of RAD51AP1 did not have a significant effect on the prognosis of AVR-CC patients (Fig. 5I). From another perspective, in patients with low RAD51AP1 expression, the prognosis of CC was significantly better than that of AVR-CC, while there was no significant difference in the prognosis of CC and AVR-CC patients with high RAD51AP1 expression (Fig. 5I). These results suggested that there may be an interaction between viral HBV status and RAD51AP1 expression concerning OS in patients with HBV-associated HCC. Taken together, HBV infection may significantly amplify the LINC01419/miR-8070/RAD51AP1 axis through a positive feedback loop in HBV-associated HCC cells and may affect the prognosis of HBV-associated HCC patients.

4.5. The LINC01419/miR-8070/RAD51AP1 axis synergizes with HBV to promote HCC cells proliferation

The CCK-8 assay indicated that overexpression of LINC01419 promoted the proliferation of HepG2 and HepG2.2.15 cells (Fig. 6A and B), and miR-8070 mimic can attenuate the promoting effect in HepG2.2.15 cells (Fig. 6C), suggesting that the LINC01419/miR-8070/RAD51AP1 axis may regulate HCC cell proliferation. Cell cycle analysis also showed that overexpression of LINC01419 in HepG2.2.15 and HepG2 cells increased the proportion of cells in the S phase (Fig. 6D–F). In addition, overexpression of LINC01419 significantly increased the proportion of cells in the S phase in HepG2.2.15 compared to HepG2 (Fig. 6F). Regarding the effect of HBx on the proliferation of HCC cells, overexpression of HBx in HepG2 cells significantly promoted cell proliferation (Fig. 6G).

In order to determine whether HBV replication and the LINC01419/miR-8070/RAD51AP1 axis synergistically promote proliferation in HBV-associated HCC cells, HepAD38, which selectively expresses HBV, was used in this experiment. As shown in Fig. 6H, overexpression of LINC01419 in HepAD38 cells also promoted cell proliferation, but the promoting effect of LINC01419 on cell proliferation was more significant in HepAD38-Tet (−) cells compared to HepAD38-Tet (+) cells. In contrast, LINC01419 knockdown inhibited HepAD38 cell proliferation, and LINC01419 knockdown inhibited HepAD38-Tet (+) cell proliferation more significantly than HepAD38-Tet (−) cells. (Fig. 6I). Taken together, the above results suggest that HBV and LINC01419/miR-8070/RAD51AP1 axis may have a synergistic effect on the proliferation of HBV-HCC cells. EdU, a thymine deoxyribonucleoside analog, can be incorporated into newly synthesized DNA by substituting for thymine deoxyribonucleoside during DNA synthesis. To further validate the role of LINC01419 in regulating cell proliferation, the EdU incorporation assay was performed to detect DNA synthesis in HBV-associated HCC cells. As shown in Supplementary Fig. S2, overexpression of LINC01419 in HepG2.2.15 and HepAD38 cells (labeled with EdU

for 6 and 1 h, respectively) significantly increased the percentage of EdU-positive cells compared to the empty vector group.

4.6. The LINC01419/miR-8070/RAD51AP1 axis synergizes with HBV to facilitate the metastasis of HBV-associated HCC cells

To further investigate the potential role of the LINC01419/miR-8070/RAD51AP1 axis in conjunction with HBV in promoting migration and invasion of HBV-associated HCC cells, wound healing and transwell assays were performed on HepAD38 Tet (−) and Tet (+) cells. As shown in Fig. 7A–F, LINC01419 in HepAD38 cells resulted in the promotion of cell metastasis, with a more pronounced effect observed in HepAD38 Tet (−) cells relative to HepAD38 Tet (+) cells, the wound closure rate and the number of metastatic cells in HepAD38 Tet (−) cells were significantly higher than those in HepAD38 Tet (+) cells. In contrast, LINC01419 knockdown in HepAD38 cells significantly suppressed cell metastasis, and the number of metastatic cells decreased significantly in both HepAD38 Tet (+) and Tet (−) cells, with a more pronounced effect observed in HepAD38 Tet (+) cells compared to HepAD38 Tet (−) cells (Fig. 7C–F). In conclusion, the above results indicate that HBV replication and the LINC01419/miR-8070/RAD51AP1 axis may have a synergistic effect on the promotion of HBV-HCC cell migration and invasion.

4.7. The LINC01419/miR-8070/RAD51AP1 axis promote HBV-associated HCC via the Wnt/β-catenin signaling pathway

To explore the mechanism by which the enhanced LINC01419/miR-8070/RAD51AP1 axis promotes HCC progression, gene set

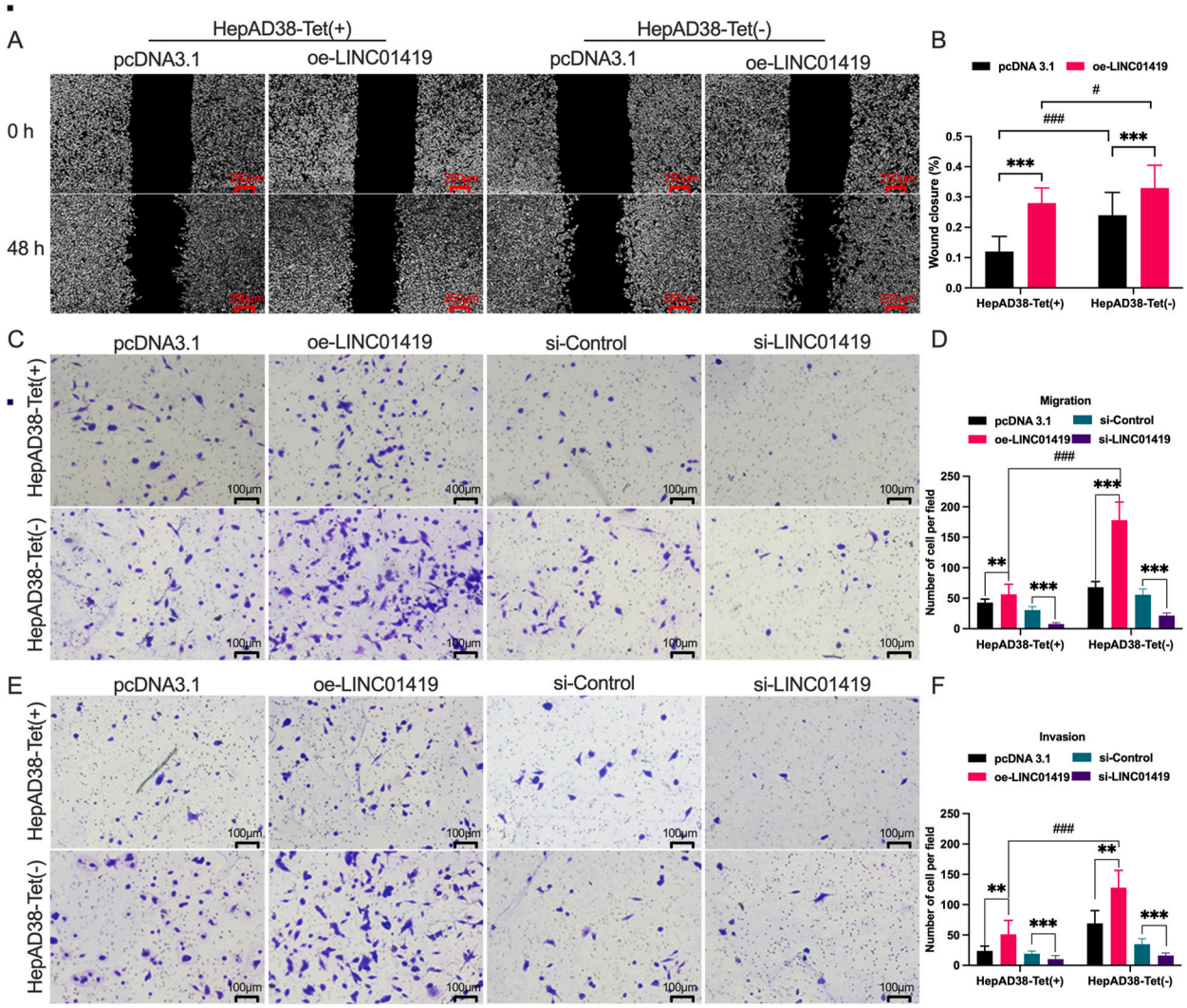

Fig. 7. The synergistic effect of LINC01419 and HBV on cell migration and invasion assay. (A–B) Wound closure assay showing the effect of LINC01419 overexpression on the migration of HepAD38 Tet (−) and Tet (+) cells compared with that of control cells transfected with control vector; (C–F) Transwell assay showing the effect of LINC01419 overexpression or knockdown on the migration and invasion of HepAD38 Tet (−) and Tet (+) cells compared with that of cells transfected with vehicle control. *P < 0.05; **P < 0.01; ***P < 0.001.

enrichment analysis (GSEA) was conducted. As illustrated in Fig. 8A, the Wnt signaling pathway was markedly enriched in the RAD51AP1 high-expression group based on the TCGA-LIHC cohort. The classical Wnt signaling pathway plays a pivotal role in the proliferation, migration, and invasion of tumor cells. Knockdown of LINC01419 or RAD51AP1, or overexpression of miR-8070 in HepG2.2.15 cells significantly increased the levels of p-β-catenin and decreased the accumulation of β-catenin in the nucleus, and downregulated the expression of its downstream target genes cell cycle proteins D1 (CCND1) and c-Myc (Fig. 8B–E), which are important biomarkers of cell proliferation and metastasis. Glycogen synthase kinase 3 beta (GSK3β) is a conserved serine/threonine protein kinase. In the absence of Wnt signaling, GSK-3β can add phosphate groups to serine/threonine residues at the N-terminus of β-Catenin, and the phosphorylated β-catenin is ubiquitylated by β-TRCP, which is degraded by the proteasome. The overexpression of miR-8070 in HepG2.2.15 cells resulted in a significant increase in the levels of GSK3β (Fig. 8D and E). In addition, phosphorylation at Ser9 (p-GSK-3β Ser9) has been shown to inhibit GSK3β activity, leading to a stable accumulation of non-phosphorylated β-catenin [13, 14]. Most of the previous studies have used the alteration of p-Gsk-3β Ser9 levels to characterize changes in cellular GSK3β activity [15]. Knockdown of LINC01419 or RAD51AP1 in HepG2.2.15 cells significantly decreased the level of p-GSK-3β Ser9 compared with the NC group (Fig. 8B and C), suggesting that knockdown of LINC01419 or RAD51AP1 may be able to enhance GSK3β activity. In contrast, LINC01419 overexpression in HepG2.2.15 cells resulted in a decrease in GSK-3β and an increase in the accumulation of β-catenin in the nucleus (Fig. 8F and G). The effects of LINC01419 overexpression were reversed by the miR-8070 mimic (Fig. 8H and I). The results indicate that the enhanced LINC01419/miR-8070/RAD51AP1 axis may promote the progression of HBV-associated HCC by enhancing the Wnt/β-catenin signaling pathway.

5. Discussion

Hepatocellular carcinoma is one of the most severe malignancies, posing a considerable threat to human health worldwide. HBV

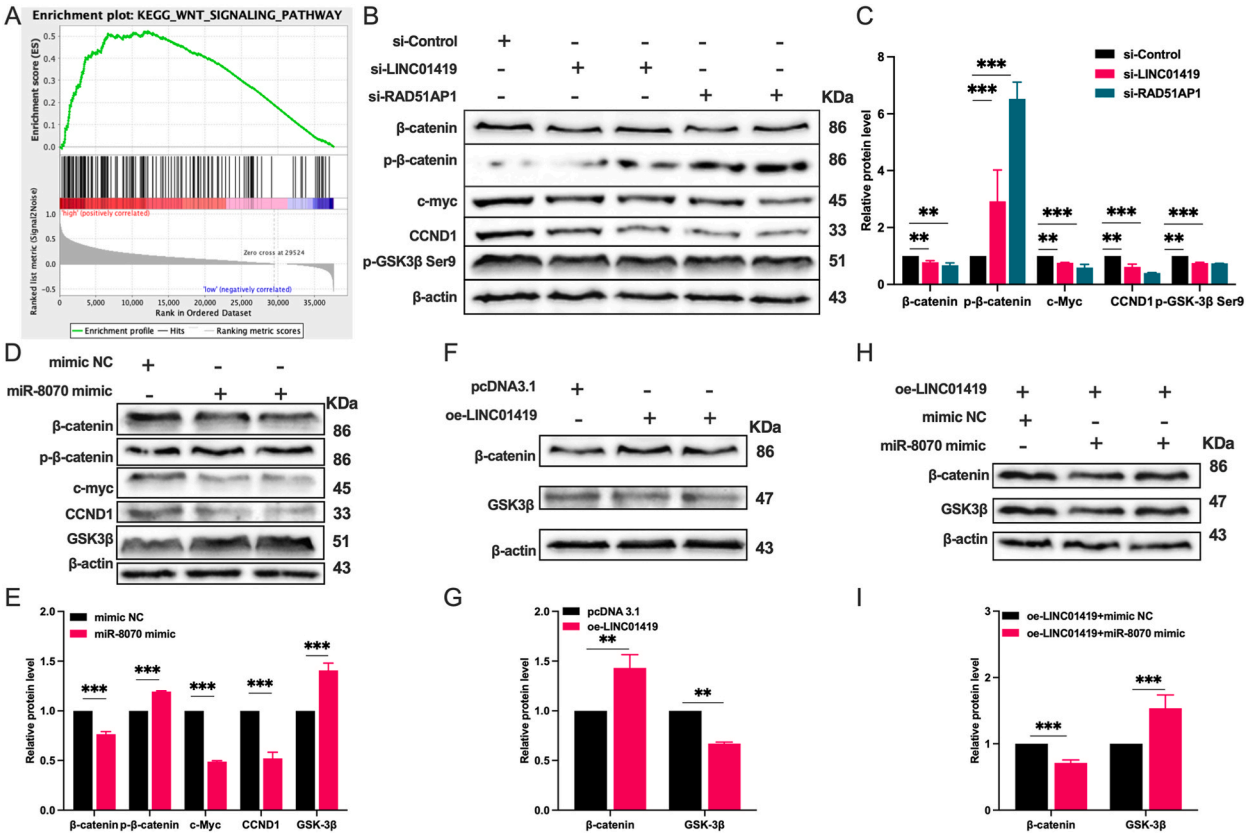

Fig. 8. The LINC01419/miR-8070/RAD51AP1 Axis activity the Wnt/β-catenin signaling pathway in HBV-associated HCC.
(A) Enriched Wnt/β-catenin signaling pathway positively correlated with RAD51AP1. (B, C) Protein levels of β-catenin, p-β-catenin, p-GSK3β, and downstream target genes CCND1 and c-Myc in HepG2.2.15 cells transfected with si-LINC01419, si-RAD51AP1 or negative control (NC) were analyzed by Western blotting analysis. (D, E) Protein levels of β-catenin, p-β-catenin, p-GSK3β, and downstream target genes CCND1 and c-Myc in HepG2.2.15 cells transfected with miR-8070 mimic or negative control (NC) were analyzed by Western blotting analysis. (F, G) Protein levels of β-catenin and GSK3β in HepG2.2.15 cells transfected with oe-LINC01419 or control vector were analyzed by Western blotting analysis. (H, I) Protein levels of β-catenin and GSK3β in LINC01419 overexpressing HepG2.2.15 cells transfected with miR-8070 mimic or negative control were analyzed by Western blotting analysis. *P < 0.05; **P < 0.01; ***P < 0.001.

infection is closely related to the incidence and development of HCC. Several studies have demonstrated that antiviral therapy can reduce the risk of HCC development in patients with chronic HBV infection and that long-term use of antiviral drugs can reduce the incidence of HCC. Antiviral therapy has also been shown to prolong OS and progression-free survival (PFS) in patients with HBV-associated HCC [16]. Identifying key driving genes is essential for the development of new and effective treatment strategies for HBV-associated HCC, ultimately improving the prognosis. In the present study, based on data from the GEO and TCGC databases, we identified RAD51AP1 as the most significant prognostic factor for OS of patients with HBV-associated HCC (HR = 1.522, 95%CI: 1.313–1.764, $p < 0.001$), and promoted HBV-associated HCC progression through the HBV-enhanced LINC01419/miR-8070/RAD51AP ceRNA axis and Wnt/β-catenin signaling pathway.

RAD51AP1 is a vertebrate-specific protein that plays a critical role in homologous recombination by activating the RAD51 recombinase [14]. Steady-state expression of RAD51AP1 is critical for maintaining genome stability. A systematic pan-cancer analysis demonstrated that RAD51AP1 is upregulated in various cancers, and is associated with the immune microenvironment, tumor stemness, and prognosis [17]. RAD51AP1 knockdown has been shown to suppress the progression of ovarian cancer [18], non-small cell lung cancer [19], pancreatic cancer [17], and esophageal squamous cell carcinoma (ESCC) [20]. Furthermore, the expression level of RAD51AP1 correlated with tumor sensitivity to radiotherapy or chemotherapy in some neoplasms [21]. For example, RAD51AP1 knockdown increased the sensitivity of colorectal cancer to chemotherapy [22], but RAD51AP1 overexpression was not sufficient to confer resistance to chemotherapy in glioma cells [23]. In HCC, Zhang et al. found that up-regulation of RAD51AP1 contributed to intrahepatic metastasis, vascular invasion, advanced tumor stage, and elevated AFP level, which was significantly associated with OS and DFS in patients with HCC by mining the TCGA and GSE36376 datasets [24]. In the present study, we further performed a subgroup analysis in patients with or without HBV-associated HCC and found that RAD51AP1 only served as a risk factor in patients with HBV-associated HCC, but had no significant effect on OS in HCC patients without HBV, our founds indicated that this gene could have a more pronounced clinical significance in patients with HBV-associated HCC. In terms of the mechanism, we found that the lncRNA LINC01419 was aberrantly highly expressed in HBV-associated HCC and was able to sponge miR-8070 to enhance the expression of RAD51AP1, i.e., LINC01419/miR-8070/RAD51AP1 constitutes a potential ceRNA regulatory axis. And, the upregulation of the LINC01419 and RAD51AP1, and the silencing of miR-8070, facilitated the malignant phenotype of HBV-associated HCC cells, which is consistent with previous reports [11,24–26].

LINC01419 has been identified as an oncogene in lung adenocarcinoma, ESCC, HCC, and gastric cancer [27–29]. In HCC, LINC01419 mediates ZIC1 epigenetic silencing to promote HCC metastasis through the PI3K/Akt signaling pathway and may serve as a diagnostic marker and potential therapeutic target for HCC [30–32]; Zhang, H.H. et al. demonstrated that LINC01419 is significantly overexpressed in HBV-associated and HCV-associated HCC and can regulate cell cycle activity to promote tumor growth [33], these findings suggesting that LINC01419 plays a critical role in promoting the malignant progression of HBV-associated HCC. The results of

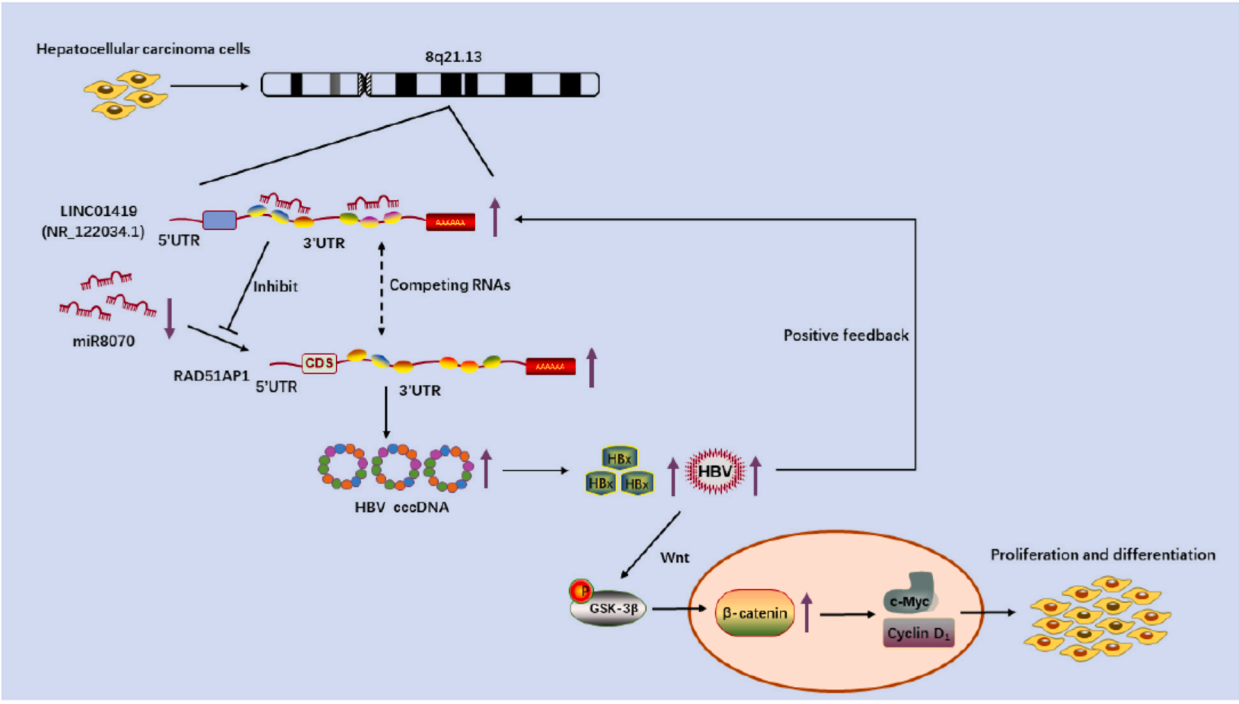

Fig. 9. Mechanism of synergy between the LINC01419/miR-8070/RAD51AP1 axis and HBV in HBV-associated HCC. As a ceRNA, LINC01419 competitively binds to miR-8070, leading to the upregulation of RAD51AP1, which stimulates the increase of HBV cccDNA and promotes HBV replication. HBV replication in turn enhances the ceRNA axis, forming a positive feedback loop that activates the Wnt/β-catenin signaling pathway and promotes the development of HCC.

this study showed that, on the one hand, HBV infection enhanced LINC01419 expression in HBV-associated HCC cells and, on the other hand, we observed significantly increased levels of cccDNA, pgRNA, and HBx in HBV-associated HCC cells with high LINC01419 expression, which suggests that LINC01419 may promote the replication of HBV. In terms of function, LINC01419 was shown to promote the proliferation, migration, and invasion of HCC cells, with these effects being more pronounced in the presence of HBV in HCC cells. The depletion of HBV or the elimination of LINC01419 was shown to attenuate these promoting effects, indicating the potential for positive feedback regulation between LINC01419 expression and HBV replication, which may contribute to the progression of HBV-associated HCC. This may partly explain the promotion of HCC progression by HBV infection and the improved prognosis of patients with HBV-associated HCC by anti-HBV therapy. However, whether aggressive anti-HBV therapy combined with LINC01419 or RAD51AP1-targeted therapy can improve the prognosis of patients with HBV-associated HCC and the exact mechanism of the positive feedback regulation between LINC01419 expression and HBV replication still needs further investigation.

The Wnt/β-catenin signaling pathway is closely associated with the initiation, progression, stemness, and drug resistance of HCC [34,35], and aberrant activation is observed in approximately 66 % of patients with HCC [36]. Various molecules, including HBV and HCV, can activate the Wnt/β-catenin pathway in HCC cells [37,38]. HBV (particularly HBx) can maintain β-catenin activation through various mechanisms and is closely associated with the expression of downstream CCND1 and c-Myc [39]. Thus, HBV replication may be a key driver of HBV-associated HCC progression through the Wnt/β-catenin signaling pathway. In the present study, the knockdown of LINC01419 or RAD51AP1 attenuated the activation of the Wnt/β-catenin signaling pathway, whereas overexpression of miR-8070 facilitated the activation of the pathway in HepG2.2.15 cells, suggesting that the LINC01419/miR-8070/RAD51AP1 axis can also enhance the Wnt/β-catenin signaling pathway. Considering the possible positive feedback regulation between LINC01419 expression and HBV replication as described above, it can be speculated that the LINC01419/miR-8070/RAD51AP1 axis and HBV may jointly promote the proliferation and metastasis of HBV-associated HCC through the Wnt/β-catenin signaling pathway (Fig. 9).

In addition, Wei et al. considered RAD51AP1 as an immune-related gene associated with the prognosis of HCC patients [11]. Given the significant difference in the effect of RAD51AP1 on OS in HCC patients with and without HBV infection, we also compared the differences in the immune microenvironment between HCC patients with different RAD51AP1 expression by the CIBERSORT algorithm. As shown in Supplementary Fig. S3, in patients with non-HBV-associated HCC, the abundance of M2-type macrophages, resting NK cells, and monocytes was significantly decreased and T follicular helper cells were significantly increased in the RAD51AP1 high expression group, whereas in patients with HBV-associated HCC, M2-type macrophages, naive B cells and CD8 T cells were significantly decreased and T follicular helper cells, memory B cells and Mø macrophages were significantly increased in the RAD51AP1 high expression group. These differences indicate that HBV infection and RAD51AP1 expression may reshape the immune microenvironment of HBV-associated HCC and ultimately lead to different outcomes. However, these mechanisms remain unclear.

6. Conclusions

In this study, we identified key genes associated with the progression of HBV-associated HCC and found a potential positive feedback loop between the LINC01419/miR-8070/RAD51AP1 axis and HBV replication, which synergistically promotes the proliferation and metastasis of HBV-associated HCC via Wnt/β-catenin signaling pathway. Our study provides new insights into the mechanism by which the LINC01419/miR-8070/RAD51AP1 axis promotes HBV-associated HCC and may provide new diagnostic and therapeutic targets for patients with HBV-associated HCC.

CRediT authorship contribution statement

Meiling Wan: Writing – original draft, Validation, Investigation, Formal analysis. **Yonghong Wang:** Resources, Data curation. **Xiaoling Liu:** Project administration. **Yaling Li:** Funding acquisition. **Cunliang Deng:** Project administration. **Changfeng Sun:** Writing – review & editing, Methodology, Conceptualization.

Ethics approval and consent to participate

Review and/or approval by an ethics committee was not needed for this study because it involved re-analysis of publicly available documents.

Availability of data and materials

All relevant data are available from the corresponding author upon reasonable request.

Declaration of generative AI and AI-assisted technologies in the writing process

The authors declare that they have not used generative AI and AI-assisted technologies in the writing process.

Abbreviation

(*continued on next page*)

(*continued*)

Abbreviation	Meaning
Abbreviation	Meaning
HCC	Hepatocellular carcinoma
HBV	Hepatitis B virus
WGCNA	Weighted gene co-expression network analysis
OS	Overall survival
TCGA	The Cancer Genome Atlas
GEO	Gene Expression Omnibus
DEG	Differentially expressed genes
PPI	Protein-protein interaction
DFI	Disease-free interval
ICGC	International Cancer Genome Consortium
DMEM	Dulbecco's modified Eagle's medium
MEM	Minimum essential medium
FBS	Fetal bovine serum
SDS-PAGE	Sodium dodecyl sulfate-polyacrylamide gel electrophoresis
PVDF	Polyvinylidene difluoride
CCK-8	Cell counting kit-8
PBS	Phosphate buffer solution
EdU	5-ethynyl-2-deoxyuridine
PI	Propidium Iodide
ANOVA	Analysis of variance
DElncRNA	Differentially expressed lncRNA
HR	Hazard ratio
cccDNA	Covalently closed circular DNA
pgRNA	Pregenomic RNA
ORF	Open reading frame
CC	Chronic carriers
AVR-CC	Active viral replication chronic carriers
PFS	Progression-free survival
ESCC	Esophageal squamous cell carcinoma
CCND1	Cell cycle proteins D1
GSK-3β	Glycogen synthase kinase 3 beta
NC	Negative control
Tet	Tetracycline
GSEA	Gene set enrichment analysis

Funding

Sichuan Provincial Science and Technology Program Joint Innovation Special Project (2022YFS0625-2B).

Declaration of competing interest

The authors declare that they have no competing interests.

Acknowledgments

We would like to thank Southwest Medical University for providing experimental sites and equipment.We would like to express our gratitude for the funding of our parent project – Sichuan Science and Technology Program (2022YFS0625).

Appendix A. Supplementary data

Supplementary data to this article can be found online at https://doi.org/10.1016/j.heliyon.2024.e41594.

References

[1] H. Sung, J. Ferlay, R.L. Siegel, M. Laversanne, I. Soerjomataram, et al., Global cancer statistics 2020: GLOBOCAN estimates of incidence and mortality worldwide for 36 cancers in 185 countries, CA Cancer J Clin 71 (3) (2021) 209–249, https://doi.org/10.3322/caac.21660.

[2] A. Baecker, X. Liu, C. La Vecchia, Z.F. Zhang, Worldwide incidence of hepatocellular carcinoma cases attributable to major risk factors, Eur. J. Cancer Prev. 27 (3) (2018) 205–212, https://doi.org/10.1097/CEJ.0000000000000428.

[3] T. Akinyemiju, S. Abera, M. Ahmed, N. Alam, M.A. Alemayohu, et al., The burden of primary liver cancer and underlying etiologies from 1990 to 2015 at the global, regional, and national level results from the global burden of disease study 2015, JAMA Oncol. 3 (12) (2017) 1683–1691, https://doi.org/10.1001/jamaoncol.2017.3055.

[4] A. Villanueva, Hepatocellular carcinoma, N. Engl. J. Med. 380 (15) (2019) 1450–1462, https://doi.org/10.1056/NEJMra1713263.
[5] R. Qiang, Z. Zhao, L. Tang, Q. Wang, Y. Wang, et al., Identification of 5 hub genes related to the early diagnosis, tumour stage, and poor outcomes of hepatitis B virus-related hepatocellular carcinoma by bioinformatics analysis, Comput. Math. Methods Med. (2021), https://doi.org/10.1155/2021/9991255, 20219991255.
[6] W. Ding, Z. Zhang, N. Ye, L. Zhuang, Z. Yuan, et al., Identification of key genes in the HBV-related HCC immune microenvironment using integrated bioinformatics analysis, JAMA Oncol. (2022), https://doi.org/10.1155/2022/2797033, 20222797033.
[7] S.Y. Wang, Y.H. Huang, Y.J. Liang, J.C. Wu, Gene coexpression network analysis identifies hubs in hepatitis B virus-associated hepatocellular carcinoma, J. Chin. Med. Assoc. 85 (10) (2022) 972–980, https://doi.org/10.1097/JCMA.0000000000000772.
[8] C. Liu, Q. Dai, Q. Ding, M. Wei, X. Kong, Identification of key genes in hepatitis B associated hepatocellular carcinoma based on WGCNA, Infect. Agents Cancer 16 (1) (2021) 18, https://doi.org/10.1186/s13027-021-00357-4.
[9] M. Sha, J. Cao, Z.P. Zong, N. Xu, J.J. Zhang, et al., Identification of genes predicting unfavorable prognosis in hepatitis B virus-associated hepatocellular carcinoma, Ann. Transl. Med. 9 (12) (2021) 975, https://doi.org/10.21037/atm-21-2085.
[10] H. Zeng, Y. Hui, W. Qin, P. Chen, L. Huang, et al., High-throughput sequencing-based analysis of gene expression of hepatitis B virus infection-associated human hepatocellular carcinoma, Oncol. Lett. 20 (4) (2020) 18, https://doi.org/10.3892/ol.2020.11879.
[11] Y. Wei, C. Lan, X. Wang, X. Zhou, X. Liao, et al., RAD51AP1 as an immune-related prognostic biomarker and therapeutic response predictor in hepatocellular carcinoma, Int. J. Gen. Med. (2023) 164377–164392, https://doi.org/10.2147/IJGM.S431206.
[12] E. Michailidis, J. Pabon, K. Xiang, P. Park, V. Ramanan, et al., A robust cell culture system supporting the complete life cycle of hepatitis B virus, Sci. Rep. 7 (1) (2017) 16616, https://doi.org/10.1038/s41598-017-16882-5.
[13] D. Lin, Y. Chen, A.R. Koksal, S. Dash, Y. Aydin, Targeting ER stress/PKA/GSK-3beta/beta-catenin pathway as a potential novel strategy for hepatitis C virus-infected patients, Cell Commun. Signal. 21 (1) (2023) 102, https://doi.org/10.1186/s12964-023-01081-9.
[14] G. Fang, P. Zhang, J. Liu, X. Zhang, X. Zhu, et al., Inhibition of GSK-3beta activity suppresses HCC malignant phenotype by inhibiting glycolysis via activating AMPK/mTOR signaling, Cancer Lett. (2019) 46311–46326, https://doi.org/10.1016/j.canlet.2019.08.003.
[15] J. Jensen, E.O. Brennesvik, Y.C. Lai, P.R. Shepherd, GSK-3beta regulation in skeletal muscles by adrenaline and insulin: evidence that PKA and PKB regulate different pools of GSK-3, Cell. Signal. 19 (1) (2007) 204–210, https://doi.org/10.1016/j.cellsig.2006.06.006.
[16] Y.F. Liaw, M. Raptopoulou-Gigi, H. Cheinquer, S.K. Sarin, T. Tanwandee, et al., Efficacy and safety of entecavir versus adefovir in chronic hepatitis B patients with hepatic decompensation: a randomized, open-label study, Hepatology 54 (1) (2011) 91–100, https://doi.org/10.1002/hep.24361.
[17] R. Liu, G. Zhu, M. Li, P. Cao, X. Li, et al., Systematic pan-cancer analysis showed that RAD51AP1 was associated with immune microenvironment, tumor stemness, and prognosis, Front. Genet. (2022), https://doi.org/10.3389/fgene.2022.971033, 13971033.
[18] H. Zhao, Y. Gao, Q. Chen, J. Li, M. Ren, et al., RAD51AP1 promotes progression of ovarian cancer via TGF-beta/Smad signalling pathway, J. Cell Mol. Med. 25 (4) (2021) 1927–1938, https://doi.org/10.1111/jcmm.15877.
[19] Y. Wu, H. Wang, L. Qiao, X. Jin, H. Dong, et al., Silencing of RAD51AP1 suppresses epithelial-mesenchymal transition and metastasis in non-small cell lung cancer, Thorac Cancer 10 (9) (2019) 1748–1763, https://doi.org/10.1111/1759-7714.13124.
[20] Y.Y. Hu, C.C. Ma, K.X. Ai, Knockdown of RAD51AP1 suppressed cell proliferation and invasion in esophageal squamous cell carcinoma, Discov Oncol 13 (1) (2022) 101, https://doi.org/10.1007/s12672-022-00566-2.
[21] R. Liu, M. Li, Z. Hu, Z. Song, J. Chen, [Research advances of RAD51AP1 in tumor progression and drug resistance], Zhongguo Fei Ai Za Zhi 26 (9) (2023) 701–708, https://doi.org/10.3779/j.issn.1009-3419.2023.102.34.
[22] A.E. Bridges, S. Ramachandran, K. Tamizhmani, U. Parwal, A. Lester, et al., RAD51AP1 loss attenuates colorectal cancer stem cell renewal and sensitizes to chemotherapy, Mol. Cancer Res. 19 (9) (2021) 1486–1497, https://doi.org/10.1158/1541-7786.MCR-20-0780.
[23] J. Zhou, F. Tong, J. Zhao, X. Cui, Y. Wang, et al., Identification of the E2F1-RAD51AP1 axis as a key factor in MGMT-methylated GBM TMZ resistance, Cancer Biol Med 20 (5) (2023) 385–400, https://doi.org/10.20892/j.issn.2095-3941.2023.0011.
[24] L. Zhuang, Y. Zhang, Z. Meng, Z. Yang, Oncogenic roles of RAD51AP1 in tumor tissues related to overall survival and disease-free survival in hepatocellular carcinoma, Cancer Control 27 (1) (2020) 1073274820977149, https://doi.org/10.1177/1073274820977149.
[25] H. Dang, L. Chen, P. Tang, X. Cai, W. Zhang, et al., LINC01419 promotes cell proliferation and metastasis in hepatocellular carcinoma by enhancing NDRG1 promoter activity, Cell. Oncol. 43 (5) (2020) 931–947, https://doi.org/10.1007/s13402-020-00540-6.
[26] Z.P. Sun, Z.G. Tan, C. Peng, Long noncoding RNA LINC01419 promotes hepatocellular carcinoma malignancy by mediating miR-485-5p/LSM4 axis, Kaohsiung J. Med. Sci. 38 (9) (2022) 826–838, https://doi.org/10.1002/kjm2.12566.
[27] Z.M. Cheng, S.Z. Hou, Y.B. Wu, X.D. Wang, Y. Sun, et al., LINC01419 promotes cell proliferation and metastasis in lung adenocarcinoma via sponging miR-519b-3p to up-regulate RCCD1, Biochem. Biophys. Res. Commun. 520 (1) (2019) 107–114, https://doi.org/10.1016/j.bbrc.2019.09.090.
[28] L.L. Wang, L. Zhang, X.F. Cui, Downregulation of long noncoding RNA LINC01419 inhibits cell migration, invasion, and tumor growth and promotes autophagy via inactivation of the PI3K/Akt1/mTOR pathway in gastric cancer, Therapeutic Advances in Medical Oncology 11 (2019). Artn1758835919874651 10 .1177/1758835919874651.
[29] J.L. Chen, Z.X. Lin, Y.S. Qin, Y.Q. She, Y. Chen, et al., Overexpression of long noncoding RNA LINC01419 in esophageal squamous cell carcinoma and its relation to the sensitivity to 5-fluorouracil by mediating GSTP1 methylation, Therapeutic Advances in Medical Oncology 11 (2019), https://doi.org/10.1177/1758835919838958.
[30] Y.F. Hou, K. Chen, R. Liao, Y.Z. Li, H.J. Yang, et al., LINC01419-mediated epigenetic silencing of ZIC1 promotes metastasis in hepatocellular carcinoma through the PI3K/Akt signaling pathway, Lab. Invest. 101 (5) (2021) 570–587, https://doi.org/10.1038/s41374-021-00539-z.
[31] S.Q. Zhang, S. Gao, M. Zhao, Y.X. Liu, Y.N. Bu, et al., Anti-HBV drugs suppress the growth of HBV-related hepatoma cells via down-regulation of hepatitis B virus X protein, Cancer Lett. (2017), 39294-104.
[32] H.W. Hann, R. Coben, D. Brown, L. Needleman, E. Rosato, et al., A long-term study of the effects of antiviral therapy on survival of patients with HBV-associated hepatocellular carcinoma (HCC) following local tumor ablation, Cancer Med. 3 (2) (2014) 390–396.
[33] H.H. Zhang, C.P. Zhu, Y. Zhao, M. Li, L.C. Wu, et al., Long non-coding RNA expression profiles of hepatitis C virus-related dysplasia and hepatocellular carcinoma, Oncotarget 6 (41) (2015) 43770–43778, https://doi.org/10.18632/oncotarget.6087.
[34] Y. Liu, X. Ye, J.B. Zhang, H. Ouyang, Z. Shen, et al., PROX1 promotes hepatocellular carcinoma proliferation and sorafenib resistance by enhancing beta-catenin expression and nuclear translocation, Oncogene 34 (44) (2015) 5524–5535, https://doi.org/10.1038/onc.2015.7.
[35] M. Huang, C. Chen, J. Geng, D. Han, T. Wang, et al., Targeting KDM1A attenuates Wnt/beta-catenin signaling pathway to eliminate sorafenib-resistant stem-like cells in hepatocellular carcinoma, Cancer Lett. (2017) 39812–39821, https://doi.org/10.1016/j.canlet.2017.03.038.
[36] Y. Totoki, K. Tatsuno, K.R. Covington, H. Ueda, C.J. Creighton, et al., Trans-ancestry mutational landscape of hepatocellular carcinoma genomes, Nat. Genet. 46 (12) (2014) 1267–1273, https://doi.org/10.1038/ng.3126.
[37] M. Daud, M.A. Rana, T. Husnain, B. Ijaz, Modulation of Wnt signaling pathway by hepatitis B virus, Arch. Virol. 162 (10) (2017) 2937–2947, https://doi.org/10.1007/s00705-017-3462-6.
[38] S. Aicher, A. Kakkanas, L. Cohen, B. Blumen, G. Oprisan, et al., Differential regulation of the Wnt/beta-catenin pathway by hepatitis C virus recombinants expressing core from various genotypes, Sci. Rep. 8 (1) (2018) 11185, https://doi.org/10.1038/s41598-018-29078-2.
[39] A. Hsieh, H.S. Kim, S.O. Lim, D.Y. Yu, G. Jung, Hepatitis B viral X protein interacts with tumor suppressor adenomatous polyposis coli to activate Wnt/beta-catenin signaling, Cancer Lett. 300 (2) (2011) 162–172, https://doi.org/10.1016/j.canlet.2010.09.018.